

# APPLICATION OF PERESKIA ACULEATA MILL. LEAVES POWDER FOR REMOVAL OF CD(II) AND PB(II) FROM MONO- AND BICOMPONENT SYSTEMS

Data de aceite: 03/07/2023

### **Josiane Lopes de Oliveira**

Department of Chemistry, Institute of Biological and Exact Sciences (ICEB), Federal University of Ouro Preto, Campus Morro do Cruzeiro, Bauxita, Ouro Preto, Minas Gerais, Brazil

### **Emylle Emediato Santos**

Department of Chemistry, Institute of Biological and Exact Sciences (ICEB), Federal University of Ouro Preto, Campus Morro do Cruzeiro, Bauxita, Ouro Preto, Minas Gerais, Brazil

### **Liliane Catone Soares**

Department of Chemistry, Institute of Biological and Exact Sciences (ICEB), Federal University of Ouro Preto, Campus Morro do Cruzeiro, Bauxita, Ouro Preto, Minas Gerais, Brazil

### **Roberta Eliane Santos Froes**

Department of Chemistry, Institute of Biological and Exact Sciences (ICEB), Federal University of Ouro Preto, Campus Morro do Cruzeiro, Bauxita, Ouro Preto, Minas Gerais, Brazil

**ABSTRACT:** In this work, *Pereskia aculeata* Mill. leaves were used to produce a biosorbent (OPN) to remove Cd(II) and Pb(II) from aqueous solutions. OPN was obtained according to a very simple and green process, without any need for chemical modification. The biosorbent was characterized by FTIR spectroscopy, elemental C, H, and N analysis, scanning electron microscopy, measurement of the point of zero charge pH, and determination of the number of acid functions. Batch studies of the adsorption of Cd(II) and Pb(II) as a function of solution pH were performed using single and binary aqueous solutions. The optimum pH for the adsorption of both ions on OPN was pH 5.0, resulting in adsorption capacities of 95 mg g<sup>-1</sup> and 27 mg g<sup>-1</sup> for Pb(II) and Cd(II), respectively. The reuse of OPN was evaluated and it was shown that the use of 0.10 mol L<sup>-1</sup> HNO<sub>3</sub> solution enabled almost complete desorption of both cations.

**KEYWORDS:** Raw material, wastewater treatment, biosorption, inorganic contaminants, cadmium, lead.

## 1 | INTRODUCTION

Cadmium and lead are metals with high toxicity. According to the priority list of hazardous substances published by the Agency for Toxic Substances and Disease Registry (ATSDR), lead is the second most hazardous substance, while cadmium occupies the seventh position on this list (ATSDR, 2019). These metals do not perform any nutritional or biochemical functions in microorganisms, plants, or animals. Their presence in living organisms is highly harmful, even at low concentrations (Kim et al., 2015).

Due to the significant threat of anthropogenic pollution to water resources, effective control of toxic metal pollution is increasingly necessary (Li et al., 2019). Technologies and methods such as physicochemical processes of chemical precipitation, evaporation and concentration, ion exchange, reverse osmosis, electrodialysis, and adsorption have been commonly used to remove toxic metal ions from wastewater (Mi et al., 2012). However, in most cases, these methods are not suitable for the decontamination of large volumes of effluents, due to low operational efficiency and high extraction costs (Volesky, 2001). Therefore, it is essential to search for alternative methods that are both highly efficient and inexpensive, and that generate low amounts of toxic waste at the end of water treatment processes.

Biosorption is defined as the phenomenon in which certain ions or molecules in aqueous solutions bind and concentrate on the surfaces of biological materials such as living or dead microorganisms, algae, plant materials, and industrial and agricultural wastes, among others (Fomina and Gadd, 2014). This process has been widely used to remove organic and inorganic contaminants from aqueous solutions. It is based on multiple physicochemical mechanisms, including absorption, ion exchange, surface complexation, and precipitation. It is a cost-effective, highly efficient (Vanhoudt et al., 2018), and more environmentally friendly method for producing high-quality effluents, while consuming fewer toxic chemicals, resulting in less toxic sludge at the end of the process (Zhao, 2011).

*Pereskia aculeata* Mill., a plant of the *Cactaceae* family (Butterworth and Wallace, 2005), popularly known as Barbados gooseberry in English (Martin et al., 2017) and as ora-pro-nobis (OPN) in Portuguese, is an unconventional food plant common in Brazil (Cruz et al., 2021). OPN is easy to cultivate in regions with temperatures above 25 °C and high incidence of sunlight (Maciel et al., 2020). This species of cactus has a high content of proteins and mineral elements such as iron, manganese, zinc, and calcium (Maciel et al., 2018), which makes it an excellent option as an ideal supplement for the human diet (Neves et al., 2020).

In addition to nutritional potential, OPN leaves are rich in a non-toxic mucilage composed of the type I arabinogalactan biopolymer, linked to protein components (Neves et al., 2020; Oliveira et al., 2019), which has biological activities and potential applications in pharmaceutical, industrial, medicinal, and food processes (Maciel et al., 2018).

The high content of carbohydrate polymers found in *P. aculeata* is an interesting feature, given that the presence of hydroxide, carboxyl, or nitrogen groups can play an important role in binding metal cations, making this material an attractive option for use in the removal of potentially toxic cations from aqueous solution. Furthermore, OPN is a biodegradable and renewable material with low economic value, which contributes to making it suitable for application in methodologies that are more accessible.

Several recent studies concerning Cd(II) and Pb(II) removal have investigated the performance of alternative materials that offer sustainability, availability in large quantities, and low cost, such as marine green algae (Bulgariu and Bulgariu, 2016), banana stalk, corn cob, and sunflower achene (Mahmood-ul-Hassan et al., 2015), jatoba (*Hymenaea courbaril*) fruit shell (Souza et al., 2017), *Dicerocaryum eriocarpus* plant mucilage (Jones et al., 2016), biochar derived from poplar sawdust (Cheng et al., 2021), kiwi branch (Tan et al., 2022), and tobacco stem (Zhou et al., 2018). However, for these materials to have a high removal capacity, a chemical modification stage is required, which increases the cost of the biosorbent and often involves using toxic chemicals. Therefore, the present study is significant not only for the use of a low-cost, sustainable, and biodegradable adsorbent, but also for achieving high removal capacity without any need for chemical modification pretreatment of the material.

This work describes the use of dried raw biomass as a biosorbent to remove toxic metal cations from mono- and bicomponent systems, at different pH values. The biosorbent was characterized by elemental C, H, and N analysis, Fourier transform infrared spectroscopy (FTIR), and scanning electron microscopy (SEM). The point of zero charge (PZC) and the number of acidic sites in the material were also determined.

## 2 | MATERIALS AND METHODS

### 2.1 Biosorbent production

Ora-pro-nobis (*P. aculeata*) leaves were collected in Canaã (Minas Gerais state, Brazil). The leaves were washed using tap water and then deionized water (deionizer model ORBC 30A, BFilters). After draining the excess water, the material was dried in an oven (model 315 SE, Fanem) at  $(60.0 \pm 0.5) ^\circ\text{C}$ , until constant weight. The dried leaves were ground using a vertical rotor micro mill (model MA048, Marconi) coupled to a 20-mesh sieve, to obtain OPN powder with homogeneous particles.

### 2.2 Biosorbent characterization

The surfaces of OPN and OPN loaded with Cd(II) (OPN-Cd) and Pb(II) (OPN-Pb) were analyzed by scanning electron microscopy (SEM) and energy dispersive X-ray spectroscopy (EDX), using a Tescan Vega3 SB electron microscope with a tungsten filament,

operating with an acceleration voltage of 20 kV, secondary electron detector, and electron backscattering. The sample was deposited on double-sided carbon tape, which was fixed on an aluminum sample holder, followed by coating (twice) with gold using a modular high-vacuum coating system (model Q150RES, Quorum Technologies).

The thermal stability of OPN was studied by heating 20 mg portions of the material between 25 and 900 °C, at a rate of 10 °C min<sup>-1</sup>, under an atmosphere of synthetic air supplied at a flow rate of 20 mL min<sup>-1</sup>. These analyses employed a thermal analyzer (model 60H, Shimadzu) and alumina crucible sample holders.

Fourier transform infrared spectroscopy (FTIR) with attenuated total reflectance (ATR) was used to identify the main OPN functional groups involved in the biosorption of metal ions. The spectra were acquired between 400 and 4000 cm<sup>-1</sup>, with 32 scans per sample, using an FTIR spectrophotometer (model MB3000, ABB Bomem, Quebec, Canada).

The carbon, hydrogen, and nitrogen contents in the adsorbent material were determined by elemental analysis (2400 CHNS/O Series II Analyzer, PerkinElmer).

The coordination number (*CN*) for the complexes formed with Cd(II) or Pb(II), together with the total number of acid functions ( $n_{H^+}$ ) of OPN, were obtained as described by Elias et al. (2022). The  $n_{H^+}$  value was determined by acid-base titration (Teodoro, 2016). For this, a 100.0 mL volume of standardized sodium hydroxide solution (0.01 mol L<sup>-1</sup>) was added to a 125 mL Erlenmeyer flask containing (0.1000 ± 0.0001) g of the adsorbent. The system was kept under constant magnetic agitation (SP-Labor stirrer) at 300 rpm for 60 min, at room temperature. The mixture was then subjected to simple filtration using a cellulose filter (type GR 418X10IN, Whatman). A 25.00 mL aliquot of the filtrate was titrated with a standardized solution of hydrochloric acid (0.01 mol L<sup>-1</sup>), using an alcoholic solution of phenolphthalein as indicator. The  $n_{H^+}$  value was calculated according to **Equation 1**.

$$n_{H^+} = \frac{(C_{NaOH} \cdot V_{NaOH}) - (C_{HCl} \cdot V_{HCl}) \cdot f}{m} \quad (1)$$

where,  $C_{NaOH}$  and  $C_{HCl}$  are the concentrations (mmol L<sup>-1</sup>) of the standardized solutions of NaOH and HCl, respectively,  $V_{NaOH}$  is the titrated volume (mL),  $V_{HCl}$  is the volume (mL) of the standardized HCl solution,  $m$  is the mass (g) of the adsorbent, and  $f$  is a correction factor (100/25).

The point of zero charge (pH<sub>PZC</sub>) was determined following the methodology described by Noh and Schwarz (1990). Solutions of NaNO<sub>3</sub> (0.01 mol L<sup>-1</sup>) were adjusted to pH 3.0, 4.5, and 6.5 by adding sodium hydroxide and/or nitric acid solutions (both at 0.1 mol L<sup>-1</sup>). Aliquots of 25.00 mL of each solution with adjusted pH were then transferred to 125 mL Erlenmeyer flasks containing different amounts of the adsorbent material (0.2000, 0.1000, 0.0500, and 0.0200 g). The mixtures were kept for 24 h at room temperature, in an incubator with constant orbital agitation at 130 rpm. The final pH of each solution was then measured (KASVI pH meter). The pH<sub>PZC</sub> was obtained at the convergence point of the three curves.

### 2.3 Assays of Cd(II) and Pb(II) adsorption on OPN

Adsorption experiments were performed, in duplicate, using a shaker-incubator (MA 420/B-125/E), by transferring (0.0500 ± 0.0001) g amounts of OPN into 125 mL Erlenmeyer flasks containing 50.00 mL of Cd(II) and/or Pb(II) solution (**Table 1**). The initial pH of all the solutions was adjusted by adding drops of aqueous 0.1 mol L<sup>-1</sup> HCl or 0.1 mol L<sup>-1</sup> NaOH solutions. The flasks were kept under constant agitation (130 rpm) at (26 ± 1) °C for 16 h. After this period, the samples were filtered using cellulose filter paper (GR 418X10IN, Whatman) and the filtrate was collected.

The adsorption was evaluated for monocomponent systems, as a function of solution pH, and for bicomponent systems, as a function of solution pH for two different concentrations of Cd(II) and Pb(II), in order to evaluate the influence of cation concentration on cation competition. The experimental conditions for all the adsorption experiments are shown in **Table 1**. The concentrations of Cd and Pb in solution were determined by flame atomic absorption spectrometry (FAAS), using a Varian SpectrAA 50B spectrophotometer.

| Parameter                            | Initial solution pH |               |                   |      |
|--------------------------------------|---------------------|---------------|-------------------|------|
|                                      | Monocomponent       | Bicomponent I | Bicomponent II    |      |
|                                      | Cd(II)              | Pb(II)        | Pb(II) and Cd(II) |      |
| Initial pH                           | 1.5 – 6.0           | 2.0 – 5.5     | 1.5 – 5.0         |      |
| Concentration / mmol L <sup>-1</sup> | 0.75                | 0.75          | 0.75              | 2.00 |

**Table 1.** Experimental conditions used for bath adsorption of Cd(II) and Pb(II) on OPN.<sup>1</sup>

<sup>1</sup>26 ± 1 °C, 16 h, 130 rpm, 1.0 g L<sup>-1</sup> of OPN.

The metal ion removal percentages (%*R*) and the amounts of metal ions adsorbed by OPN at equilibrium (*q<sub>e</sub>*, mmol L<sup>-1</sup>) were determined using **Equation 2** and **Equation 3**, respectively.

$$\%R = \frac{C_0 - C_e}{C_0} \times 100 \quad (2)$$

$$q_e = \frac{V(C_0 - C_e)}{m} \quad (3)$$

where, *C<sub>0</sub>* and *C<sub>e</sub>* (mmol L<sup>-1</sup>) are the initial and equilibrium adsorbate concentrations, respectively, *V* (L) is the solution volume, and *m* (g) is the OPN mass.

### 2.4 Reuse evaluation

The ability to reuse the OPN was evaluated in desorption assays using HNO<sub>3</sub> (0.10 mol L<sup>-1</sup>) and NaNO<sub>3</sub> (0.10 mol L<sup>-1</sup>) solutions and deionized water as eluents. Aliquots of 50.0 mL of an equimolar bicomponent solution (0.75 mmol L<sup>-1</sup>) of Cd(II) and Pb(II), at pH 5.0, were added to 125 mL Erlenmeyer flasks containing (0.0500 ± 0.0001) g of OPN. The systems were kept under the same conditions of temperature, agitation, and contact time described

in **Section 2.3**. Subsequently, the loaded adsorbent was separated by simple filtration using cellulose filter paper (GR 418X10IN, Whatman) and dried in an oven with air circulation and renewal (model TE-394/1, TECNAL), at  $(40.0 \pm 0.5)$  °C, until constant weight.

In the next step,  $(0.0500 \pm 0.0001)$  g of the dry material loaded with both Cd(II) and Pb(II) was added to 50.0 mL of each eluent solution and the systems were kept under the same conditions of temperature, agitation, and contact time described in **Section 2.3**. Once again, the materials were filtered by simple filtration and the concentrations of Cd and Pb in the solutions were determined by FAAS (SpectrAA 50B spectrophotometer, Varian). The desorption percentage was obtained according to **Equation 4**.

$$\%Desorption = \frac{\text{amount of } M(II) \text{ released}}{\text{amount of } M(II) \text{ adsorbed}} \times 100 \quad (4)$$

## 3 | RESULTS AND DISCUSSION

### 3.1 Biosorbent characterization

The elemental analysis showed that OPN was composed of  $(40 \pm 1)\%$  C,  $(4.8 \pm 0.4)\%$  H, and  $(3.8 \pm 0.3)\%$  N. The presence of a large quantity of nitrogen functions in the composition could increase the ability of OPN to remove metal cations, depending on the pH of the solution (see **Section 3.2.1**).

The SEM image of OPN (**Figure 1**) suggested that the morphology of the OPN surface was irregular, with a spongy appearance. This characteristic provided the material with a large contact area, favoring the adsorption capacity for Cd(II) and Pb(II). The EDX spectrum for OPN (**Figure 2a**) showed that among the elements present, carbon and oxygen were predominant, followed by potassium, calcium, chlorine, and magnesium. The EDX spectra of the surfaces of OPN-Cd (**Figure 2b**) and OPN-Pb (**Figure 2c**) showed clear signals for Cd and Pb, confirming the adsorption of the cations on the surface. In addition, the absence of K and Mg peaks and decreases of the Ca peaks for OPN-Cd and OPN-Pb suggested that ion exchange contributed significantly to adsorption of the metals on the OPN surface. The surface mapping SEM-EDX images for OPN-Cd (**Figure 3a**) and OPN-Pb (**Figure 3b**) suggested adsorption with saturation of the OPN surface by Cd(II) and Pb(II). Despite the saturation, it appeared that the distributions of Cd(II) and Pb(II) on the OPN surface were non-uniform.

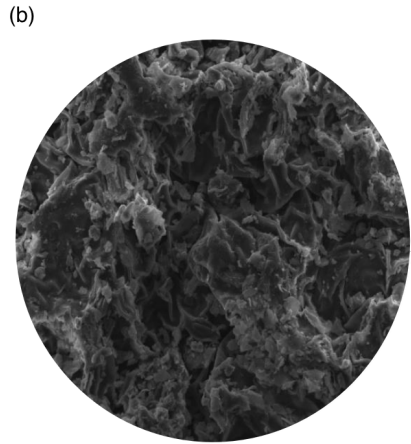
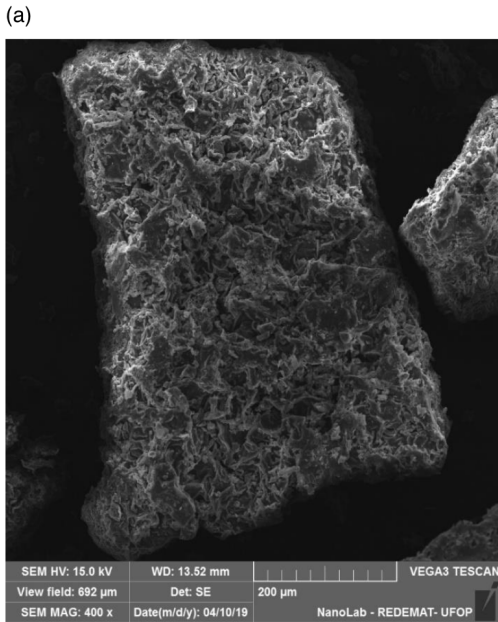


Figure 1. SEM image of OPN at (a) 400x and (b) 1000x magnification.

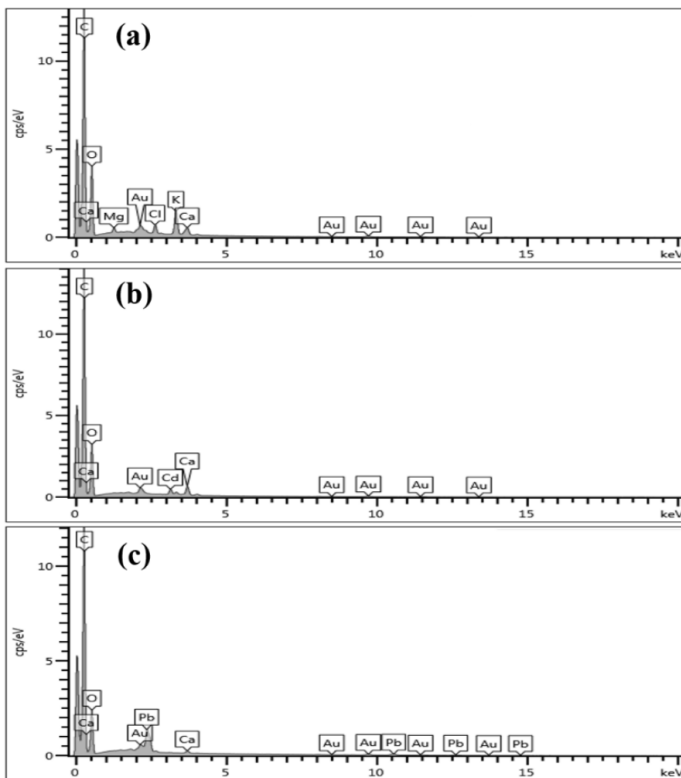


Figure 2. Elemental compositions determined by EDX peaks for (a) OPN, (b) OPN-Cd, and (c) OPN-Pb. The Au (gold) peak was due to the sputter coating.

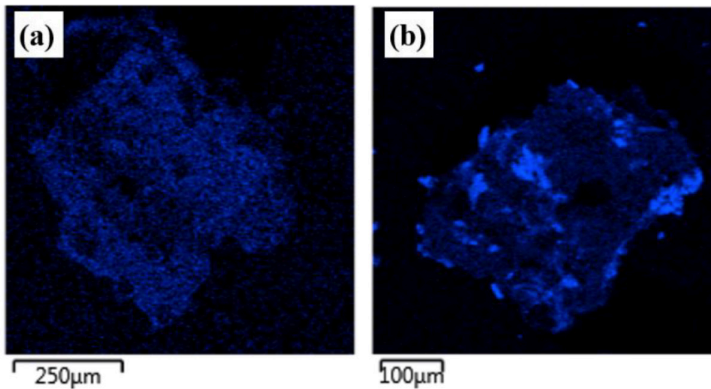


Figure 3. SEM-EDX images with surface mapping for (a) OPN-Cd and (b) OPN-Pb.

The thermogravimetric (TG) and derivative thermogravimetric (DTG) curves for OPN (**Figure 4**) suggested that the thermal decomposition occurred in at least five steps, with six significant mass loss events. The first event (at 30-120 °C) could be attributed to the loss of water physically adsorbed on the sample surface. In the range 170-400 °C, decomposition occurred in two main mass loss events ( $T_{\max} = 258.3$  and  $292.9$  °C), accounting for about 47% of the total mass loss. The event in the range 400-500 °C ( $T_{\max} = 450.2$  °C, 35% of the total weight loss) was probably related to the breaking of bonds along carbon chains or the disruption of functional groups present in the structures of polysaccharides, lipids, and proteins of OPN. The last stage of mass loss, in the range 630-900 °C ( $T_{\max} = 646.2$ ,  $734.2$ ,  $780.6$ , and  $874.8$  °C, ~6% of the total weight loss), could be explained by the breaking of the last organic chains and/or charcoal gasification (Aburto et al., 2015).

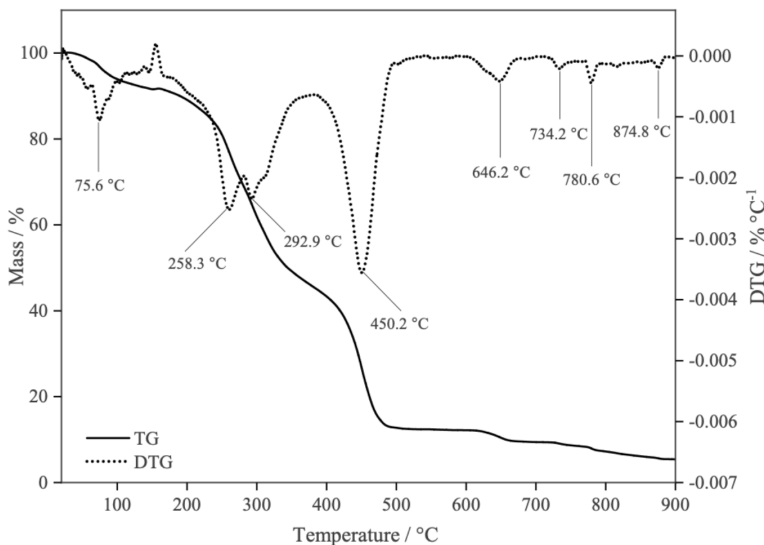


Figure 4. TG and DTG curves for the thermal decomposition of OPN.



FTIR analyses were performed before and after adsorption, in order to understand the interaction between functional groups and Cd(II) or Pb(II). The FTIR spectrum for OPN (**Figure 5**) showed an intense broad band at 3289  $\text{cm}^{-1}$ , attributed to vibrational stretching of –OH and –NH groups. Peaks at 2918 and 2850  $\text{cm}^{-1}$  corresponded to asymmetric and symmetric axial stretching of the  $-\text{CH}_2$  cluster, respectively. A band at 1731  $\text{cm}^{-1}$  could be ascribed to axial stretching vibrations of the C=O bonds of carboxylic acids or esters. A band at 1622  $\text{cm}^{-1}$  could be attributed to superposition of –NH angular deformation and C=O stretching, while stretching of the C–N bond could be observed at 1371  $\text{cm}^{-1}$ . A peak at 1315  $\text{cm}^{-1}$  corresponded to angular deformation of C–H. A low intensity band at 1240  $\text{cm}^{-1}$  was due to stretching of the carboxylic acid C–O group (Pavia et al., 2014). A low intensity peak at 1155  $\text{cm}^{-1}$  corresponded to asymmetric C–O–C stretching, related to a  $\beta$ -1-4 glycosidic bond in the polymer chain (Marques Neto et al., 2013). This bond may be associated with cellulose, a natural structural polymer that composes OPN leaves, formed by  $\beta$ -D-anhydroglucopyranose units joined by  $\beta(1 \rightarrow 4)$  glycosidic bonds (Klemm et al., 1998). A high intensity band at 1020  $\text{cm}^{-1}$  was related to symmetric C–O–C stretching (Pavia et al., 2014).

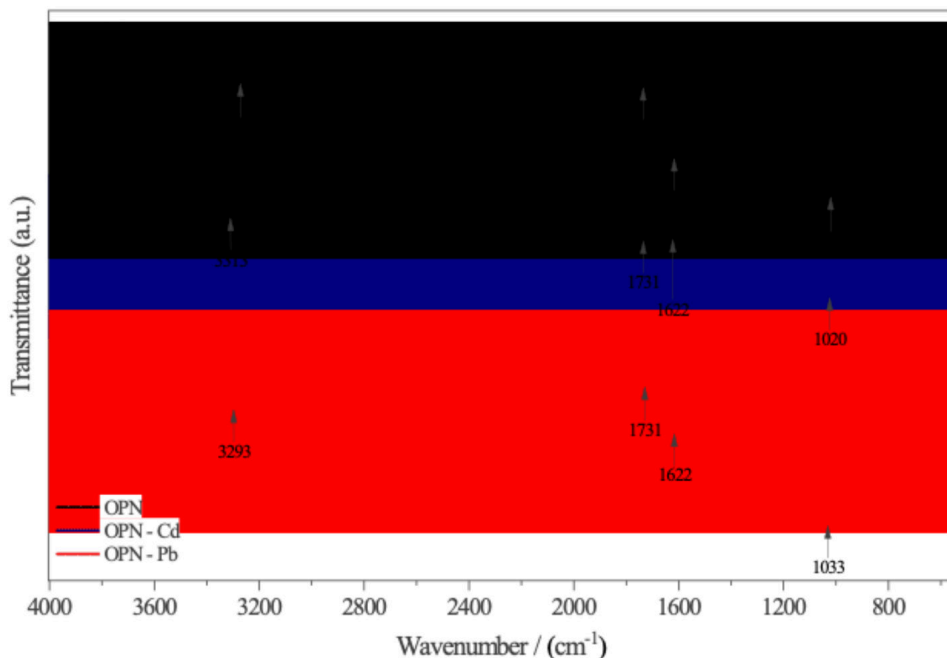


Figure 5. FTIR spectra of OPN, OPN loaded with Cd(II) (OPN-Cd), and OPN loaded with Pb(II) (OPN-Pb).

The FTIR spectra of the OPN loaded with metal ions (Cd(II) and Pb(II)) (**Figure 5**) showed that the OPN band at 3289  $\text{cm}^{-1}$  became broader and with small shifts to 3313 and 3293  $\text{cm}^{-1}$  for OPN-Cd and OPN-Pb, respectively. In the FTIR spectrum for OPN-Cd, the

peak at  $1731\text{ cm}^{-1}$  became more intense, while the strong bands at  $1622$  and  $1020\text{ cm}^{-1}$  were weakened. The FTIR spectrum for OPN-Pb showed no substantial alteration of the bands at  $1731$  and  $1622\text{ cm}^{-1}$ , while the band at  $1020\text{ cm}^{-1}$  in the original OPN spectrum increased and shifted slightly to  $1033\text{ cm}^{-1}$ . These results suggested that the nature of the predominant interaction for OPN-Cd(II) was different from that for OPN-Pb(II).

The total number of acid functions ( $n_{H^+}$ ) estimated by titration was  $(5.57 \pm 0.08)\text{ mmol g}^{-1}$ . Considering  $Q_{\text{max,Cd}} = (1.3 \pm 0.1)\text{ mmol g}^{-1}$  and  $Q_{\text{max,Pb}} = (1.17 \pm 0.08)\text{ mmol g}^{-1}$ , the *CN* values for Cd(II) and Pb(II) were around 4.8 and 4.3, respectively. Therefore, it is possible that Cd(II) and Pb(II) were in coordination with acid functions such as carboxylate groups from OPN, with the formation of tetra- and pentacoordinated complexes.

The OPN surface could be positively or negatively charged, depending on the solution pH, due to the presence of surface functional groups. The point of zero charge pH ( $\text{pH}_{\text{PZC}}$ ) is the pH value at which the total net surface charge of an adsorbent is equal to zero. The  $\text{pH}_{\text{PZC}}$  for OPN was  $6.73 \pm 0.08$ . Therefore, at pH values below 6.73, the total net charge on the material surface was positive, favoring the electrostatic adsorption of anions, while at pH above that value, the net surface charge was negative, favoring the biosorption of cations such as Cd(II) and Pb(II).

In order to avoid Cd(II) or Pb(II) precipitation as hydroxide (Pereira et al., 2020), the influence of the initial pH of the solution was investigated up to pH 6.0 and 5.5 for Cd(II) and Pb(II), respectively.

## 3.2 Assays of Cd(II) and Pb(II) adsorption on OPN

### 3.2.1 Influence of pH in a single-component system

The solution pH is one of the most important variables to consider in the removal of inorganic contaminants by adsorbents, since it influences the charge of adsorption sites with pH-dependent charge, as well as affecting metal speciation (Pereira et al., 2020). For both cations, the removal capacity was lower at low pH values ( $\text{pH} < 3$ ), with the removal efficiency increasing as the pH increased, until maximum removal was reached at pH 5 (**Figure 6a**). This behavior was expected, since with increase of the solution pH, there would be deprotonation of acid groups on the OPN surface, with consequent removal of Cd(II) and Pb(II) cations by means of the interactions with negative charges or pairs of non-binding electrons from the neutral functional groups. Therefore, this study showed that for both cations, the highest removal percentages achieved using OPN were at pH 5.0, with removal efficiencies of 31% for Cd(II) and 85% for Pb(II).

It is important to highlight that pH 5.0 is lower than the  $\text{pH}_{\text{PZC}}$  value (6.73) of OPN. However, it should be noted that  $\text{pH}_{\text{PZC}}$  is the net total charge, and that even below this pH there would exist functional groups with negative or neutral charges above  $\text{pH}_{\text{PZC}}$  (due to their *pKa* values). These groups would be able to interact with Cd(II) and Pb(II), with the formation of outer- or inner-sphere complexes.

The behaviors observed for the removal of Pb(II) and Cd(II) as a function of solution pH were similar. However, the affinity of OPN for Pb(II) was greater than for Cd(II), which could be attributed to differences in their chemical properties such as ionic radius, hydrated radius, electronegativity, and Pearson's hardness (**Table 2**).

For two cations with the same charge, such as Pb(II) and Cd(II), the electrostatic interaction with the exchange sites will be more favorable for the cation with the smaller hydration radius (Jimenez et al., 2004). This could be observed for Pb(II), since it has a hydrated radius of 4.01 Å, while the hydrated radius of Cd(II) is 4.26 Å (Nightingale, 1959). For cations with larger hydrated radius, the center of cationic charge is located further away from the surface of the adsorbent (Chen et al., 2010). Hence, for this reason, the electrostatic interaction between the surface of the OPN and the Cd(II) ions was weaker.

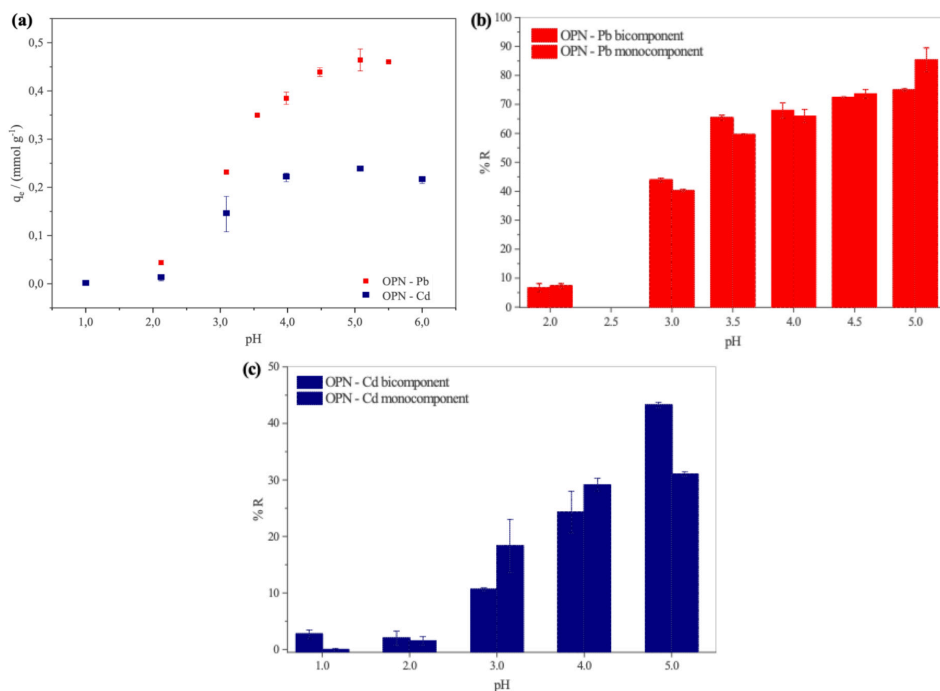


Figure 6. (a) Amounts ( $q_e$ ) of Pb(II) and Cd(II) removed in a monocomponent system, and comparison of the percentage removals of (b) Pb(II) and (c) Cd(II) in monocomponent and bicomponent systems, as a function of the initial pH of the solution. Conditions:  $(26 \pm 1) ^\circ\text{C}$ ; 16 h; 130 rpm;  $1.0 \text{ g L}^{-1}$  of OPN;  $C_0 = 0.75 \text{ mmol L}^{-1}$  for the monocomponent system;  $C_0 = 0.75$  or  $2.00 \text{ mmol L}^{-1}$  for the bicomponent system.

| Physicochemical properties | Cd        | Pb                | Reference               |
|----------------------------|-----------|-------------------|-------------------------|
| Ionic radius / Å           | 0.97      | 1.19              | Castillo et al. (2017)  |
| HSAB*                      | Soft acid | Intermediate acid | McBride (1994)          |
| Pauling Electronegativity  | 1.7       | 1.9               | Atkins and Jones (2010) |
| Hydrated radius / Å        | 4.26      | 4.01              | Nightingale (1959)      |

\* Hard Soft Acid Base theory of Pearson

Table 2. Physicochemical properties of Cd and Pb.

The lower biosorption of the Cd(II) ion could also have been related to its higher dehydration energy, compared to Pb(II), since the formation of a sphere complex requires the metallic cations to lose one or more molecules of hydration water (Sposito, 2008). Therefore, the lower the energy required for the metallic cation dehydration process to occur, the easier it is for biosorption of this species on the adsorbent surface (Petrus and Warchol, 2003; Jimenez et al., 2004).

Electronegativity is another property to consider in comparison of the biosorption of Cd(II) and Pb(II). This property can be defined as the ability of an atom to attract electrons when it is part of a compound, meaning that the greater the electronegativity of an element, the greater is its force to attract an electron (Atkins and Jones, 2010). Hence, Pb (electronegativity of 1.9) had greater strength and capacity to attract electrons from species present on the surface of the adsorbent, compared to Cd (electronegativity of 1.7). The most electronegative metals must form the strongest covalent bonds with atoms possessing non-bonding electron pairs, such as oxygen. For the bivalent metals studied, the predicted order of bond preference would be Pb > Cd. On the other hand, based on electrostatics, the strongest bond must be formed by the metal with the highest charge-radius ratio. This would produce a different order of preference for the same metals: Cd > Pb (McBride, 1994). Hence, the results suggested an important contribution of covalent bonding for the biosorption of these elements.

The greater affinity of Pb(II) for the adsorbent could also be explained by the Hard-Soft Acid-Base theory of Pearson (1990). Given that Pb(II) is a harder acid than Cd(II), it has a greater affinity for binding to most of the functional groups present in organic matter, including carboxylic groups (McBride, 1994). Therefore, this factor makes Pb(II) preferable for biosorption/complexation reactions, with formation of internal sphere complexes, when compared to Cd(II) (McBride, 1994).

The preferential bonding of metal ions can also be explained by stereochemical effects, since larger ions can adapt more easily to binding sites with two distant functional groups (Papageorgiou et al., 2006). Therefore, since Pb(II) has a larger ionic radius (1.19 Å) than Cd(II) (0.97 Å), it is better accommodated at the binding sites of distant functional groups.

Castillo et al. (2017), who studied the use of chili seed residues for individual and competitive adsorption of Pb(II) and Cd(II), also observed preferential adsorption of Pb(II), compared to Cd(II). Adsorption studies using lignin-based compounds (Guo et al., 2008; Jiao et al., 2022; Santos et al., 2022) showed that this type of matrix has greater affinity for Pb(II) ions than for Cd(II) ions. This behavior was also observed by Appel et al. (2008), who investigated the biosorption sequence of Pb(II) and Cd(II) ions in three different tropical soils. Preferential retention of Pb(II), compared to Cd(II), was observed for the three soil types, irrespective of the order in which these metal ions were added to the system.

### 3.2.2 Influence of pH in a bicomponent system

The percentage removals of Pb(II) and Cd(II) showed increasing trends as the solution pH increased, for both monocomponent (**Figure 6b**) and bicomponent (**Figures 6c** and **6d**) systems. For Pb(II), up to pH 4.5, there was no significant difference between the removal percentages for the bicomponent and monocomponent systems (**Figure 6b**), demonstrating that the presence of Cd(II) did not influence the adsorption of Pb(II) on OPN. However, at pH 5.0, the presence of Cd(II) prevented Pb(II) adsorption. For Cd(II), from pH 3.0, the removal percentage differed significantly (*t*-test, 95% confidence) between the mono- and bicomponent systems (**Figure 6c**). At pH 3.0-4.0, the presence of Pb(II) prevented Cd(II) adsorption. This antagonistic effect was expected, due to competition of the cations for the same adsorption sites. According to Serrano et al. (2005), if two or more metal ions compete for the same types of biosorption sites, the adsorption of the more strongly bound metal ion forces the more weakly adsorbed metal to be adsorbed at lower energy active sites, such as exchange sites.

However, at pH 5.0, the adsorption of Cd(II) in the bicomponent system was greater than that in the monocomponent system, indicating a synergistic effect of the presence of Pb(II) on the adsorption of Cd(II). Cooperative adsorption has already been demonstrated for several metals susceptible to hydrolysis (Sposito, 2008).

Evaluation was also made of whether the initial concentration of Pb(II) and Cd(II) ( $0.75 \text{ mmol L}^{-1}$ ) was sufficiently high to promote competition between them, because at low adsorbate concentrations there was an excess of active sites available on the OPN surface, compared to the amount of cations in solution. Therefore, the assay was also carried out in a competition system (**Figure 7**) using a higher concentration ( $2.0 \text{ mmol L}^{-1}$ ) of the two cations.

When the higher concentration of both cations ( $2.0 \text{ mmol L}^{-1}$ ) was used, only Pb(II) was adsorbed on OPN, for all the pH values tested. Therefore, in the systems with lower concentrations of both cations, the ratio between the cation concentration (adsorbate) and the adsorption sites (adsorbent) was low, so there was no substantial competition between the two cations. On the other hand, at higher concentrations, the Cd(II) adsorption percentage was close to zero, since Pb(II) had higher affinity for the OPN adsorption sites, compared to Cd(II). This could be explained by the greater number of ions competing for binding sites available on the surface of the adsorbent material (Puranik and Paknikar, 1999).

These results confirmed the previous suggestion that OPN was selective towards Pb(II). Nonetheless, the percentage of adsorbed Pb(II), ( $32 \pm 2\%$ ), was lower than found for the monocomponent system, or even for the bicomponent system with a low concentration of contaminants ( $0.75 \text{ mmol L}^{-1}$ ), indicating that the presence of Cd(II) was able to inhibit the adsorption of Pb(II). For the bicomponent system with a low initial concentration of cations

(0.75 mmol L<sup>-1</sup>), the maximum amounts of Cd(II) and Pb(II) removed were (0.232 ± 0.003) mmol g<sup>-1</sup> and (0.344 ± 0.002) mmol g<sup>-1</sup>, respectively (**Figure 7**). On the other hand, in the system with a higher concentration of cations (2 mmol L<sup>-1</sup>), the maximum amounts of Pb(II) and Cd(II) removed were (0.64 ± 0.05) mmol g<sup>-1</sup> and (0.04 ± 0.04) mmol g<sup>-1</sup>, respectively.

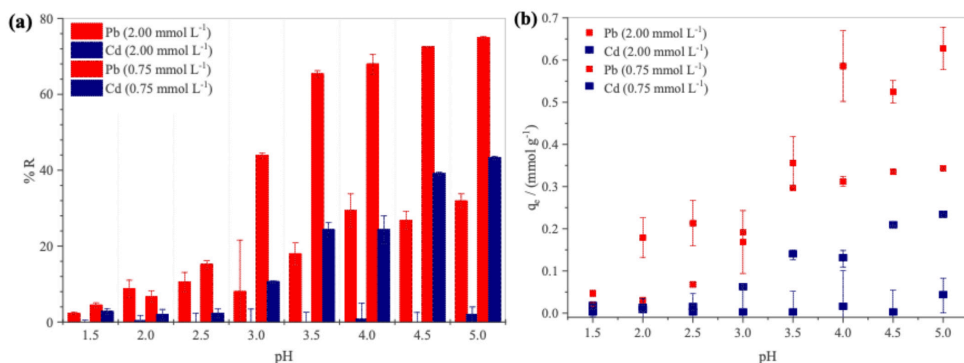


Figure 7. (a) Percentages and (b) amounts ( $q_e$ ) of Pb(II) and Cd(II) ions removed in a bicomponent system, as a function of the initial pH of the solution. Conditions: (26 ± 1) °C; 16 h; 130 rpm;  $C_0 = 0.75$  mmol L<sup>-1</sup> or 2.0 mmol L<sup>-1</sup>; 1.0 g L<sup>-1</sup> of OPN.

The decrease of the adsorption capacity for the ions could be explained by the increase of the ionic strength of the solution, as observed by Low et al. (2000), who studied the adsorption of the same cations by a biomass residue from the brewing industry. Such behavior has also been reported for other types of biosorbents, such as algae biomass (He and Chen, 2014), oilseed husks (Pehlivan et al., 2009), mineral adsorbents (Chen et al., 2011), and soils (McBride, 1994).

The pH studies showed that for both metals, the maximum adsorption capacity was obtained at pH 5.0. Therefore, pH 5.0 was established as the optimal pH (for the studied experimental conditions) and was used for the equilibrium experiment (**Section 3.2.2**).

The adsorption capacity of OPN at pH 5.0 ( $q_e = 95$  mg g<sup>-1</sup> for Pb(II) and  $q_e = 27$  mg g<sup>-1</sup> for Cd(II)) was higher than the maximum adsorption capacities reported for many natural biosorbents and even for some modified biosorbents (**Table 3**).

The OPN biosorbent could be produced according to a very simple and green process, with no need for chemical modification, and presented a high adsorption capacity for Cd(II) and Pb(II). This shows the great advantage of OPN, compared to modified adsorbents, because although chemical modification of biomass is a common method used to improve biosorbent adsorption capacity, it must be efficient, low cost, and not generate secondary pollution (Maia et al., 2021), which may be difficult to achieve in practice.

### 3.3 OPN reuse evaluation

The desorption efficiencies for Cd(II) and Pb(II) using different desorption solutions are shown in **Figure 8**. The desorption study was important for evaluation of the forces

involved in the interactions of Pb(II) and Cd(II) with the OPN adsorption sites, as well as for identification of the best desorption solution to be used for OPN reuse in further adsorption cycles.

Deionized water removed a small amount of Pb(II), ( $11.6 \pm 0.6\%$ ), but a substantial amount of Cd(II), ( $57.8 \pm 0.2\%$ ), due to the ability of deionized water to only remove those ions bonded to the adsorbent by Van der Waals interactions. The  $\text{NaNO}_3$  solution also showed higher efficiency for desorption of Cd(II) ( $(66.9 \pm 0.8\%)$ ), compared to Pb(II) ( $(37.1 \pm 0.6\%)$ ). This solution was able to remove cations adsorbed on exchange sites by electrostatic interaction.

The highest desorption percentages were achieved using  $\text{HNO}_3$  solution as eluent ( $(99.5 \pm 0.2\%)$  for Cd(II) and  $(89 \pm 3\%)$  for Pb(II)). Under acidic conditions,  $\text{H}^+$  ions protonate the surface of the adsorbent, replacing the metallic ions adsorbed on the surface, leading to desorption of adsorbed species such as positively charged metal ions (Karthikeyan et al., 2007), including those in non-exchangeable form (McBride, 1989). These results indicated that  $\text{HNO}_3$  solution was a suitable eluent for the recovery of adsorbed metal cations, enabling the adsorbent material to be reused in further cycles of cation removal.

For all the desorption solutions, the desorption efficiency was higher for Cd(II) than for Pb(II). This corroborated the results of the adsorption assays suggesting that Pb(II) adsorption occurred at higher energy sites, compared to the adsorption of Cd(II).

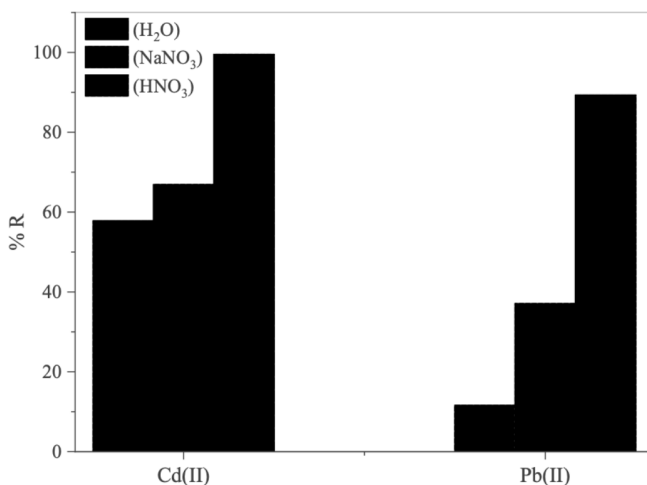


Figure 8. Desorption efficiencies for removal of Cd(II) and Pb(II) from OPN, using different desorption solutions. Conditions:  $T = (26 \pm 1) ^\circ\text{C}$ ; contact time = 16 h; agitation speed = 130 rpm;  $1.0 \text{ g L}^{-1}$  of OPN.

| Biosorbent   | $Q_{\max}^1 / \text{mg g}^{-1}$ |        | pH                       | Dosage / $\text{g L}^{-1}$ | Temperature / $^{\circ}\text{C}$ | Agitation speed / rpm | Reference                        |
|--|---------------------------------|--------|--------------------------|----------------------------|----------------------------------|-----------------------|----------------------------------|
|  | Cd(II)                          | Pb(II) |                          |                            |                                  |                       |                                  |
| Papaya peel  | -                               | 38.31  | 5.0                      | 5                          | -                                | 150                   | (Abbaszadeh et al., 2016)        |
| Seaweed <i>Posidonia oceanica</i> fibers                   | 100                             | 100    | 6.0                      | 5                          | 40                               | 300                   | (Boulaiche et al., 2019)         |
| Kiwi branch biochar  | -                               | 161.2  | 5.5                      | 0.8                        | 30                               | 200                   | (Tan et al., 2022)               |
| Modified baker's yeast ( <i>Saccharomyces cerevisiae</i> ) | 32.26                           | 200    | 5.0                      | 1                          | 25                               | 150                   | (Dutta et al., 2016)             |
| Modified <i>Syzygium cumini</i> leaf                       | 57.14                           | 109.8  | 6.0 Cd(II)<br>7.0 Pb(II) | 5                          | > 40                             | 180                   | (Salman et al., 2020)            |
| Modified residues of <i>Anacardium occidentale</i> L.      | 12.5                            | 27.1   | 5.0                      | 4                          | 25                               | 200                   | (Coelho et al., 2018)            |
| Cashew nut shell ( <i>Anacardium occidentale</i> L.)       | 11.2                            | 28.6   | 5.0                      | 12                         | 25                               | 200                   | (Coelho et al., 2014)            |
| Jatoba ( <i>Hymenaea courbaril</i> ) fruit shell           | 30.27                           | 48.75  | 5.5 Pb(II)<br>4.0 Cd(II) | 5.0                        | "room temperature"               | 180                   | (Souza et al., 2017)             |
| Modified banana stalk                                      | 6.738                           | 59.39  | -                        | 20                         | 25                               | 175                   | (Mahmood-ul-Hassan et al., 2015) |
| Modified corn cob  | 19.86                           | 56.67  | -                        | 20                         | 25                               | 175                   | (Mahmood-ul-Hassan et al., 2015) |
| Modified sunflower achene                                  | 16.282                          | 39.23  | -                        | 20                         | 25                               | 175                   | (Mahmood-ul-Hassan et al., 2015) |
| <i>Moringa oleifera</i> leaves                             | 16.13                           | 45.83  | 6.0                      | 10                         | 25                               | 150                   | (Abatal et al., 2021)            |
| <i>Moringa oleifera</i> seeds                              | 4.97                            | 49.50  | 6.0                      | 10                         | 25                               | 150                   | (Abatal et al., 2021)            |
| <i>Pennisetum glaucum</i> como                             | 5.55                            | 15.24  | 6.0                      | 2                          | 25                               | 125                   | (Yousaf et al., 2017)            |

<sup>1</sup> From Langmuir isotherm.

Table 3. Comparison of the OPN and different biosorbents reported in the literature for removal of Cd(II) and Pb(II) from aqueous solutions.

## 4 | CONCLUSIONS

*P. aculeata* leaf was successfully used to produce a green and low-cost biosorbent (OPN) with high adsorption capacities for Cd(II) and Pb(II), which exceeded those of



many similar biosorbents reported in the literature, including adsorbents produced using chemical modification. This showed the great advantage of OPN, since excellent results were achieved without any requirement for chemical modification. The best Pb(II) and Cd(II) removal efficiencies were obtained at pH 5, with OPN presenting greater affinity for Pb(II) than for Cd(II). The material could be reused after desorption using 0.10 mol L<sup>-1</sup> HNO<sub>3</sub> solution, which provided desorption efficiencies of (99.5 ± 0.2)% for Cd(II) and (89 ± 3)% for Pb(II).

## CREDIT AUTHORSHIP CONTRIBUTION STATEMENT

**Josiane Lopes de Oliveira:** Conceptualization, Methodology, Software, Formal analysis, Investigation, Visualization, Writing - original draft. **Emylle Emediato Santos:** Formal analysis, Investigation. **Liliane Catone Soares:** Conceptualization, Methodology, Formal analysis, Writing - review & editing. **Roberta Eliane Santos Froes:** Conceptualization, Writing - review & editing, Funding acquisition, Supervision, Project administration.

## ACKNOWLEDGMENTS

The authors are grateful to Universidade Federal de Ouro Preto (UFOP) and Fundação de Amparo à Pesquisa do Estado de Minas Gerais (FAPEMIG, grant number APQ 01974-17).

## REFERENCES

Abatal, M., Olguin, M.T., Anastopoulos, I., Giannakoudakis, D.A., Lima, E.C., Vargas, J., Aguilar, C., 2021. Comparison of Heavy Metals Removal from Aqueous Solution by *Moringa oleifera* Leaves and Seeds. *Coatings* 11, 508. <https://doi.org/10.3390/coatings11050508>

Abbaszadeh, S., Wan Alwi, S.R., Webb, C., Ghasemi, N., Muhamad, I.I., 2016. Treatment of lead-contaminated water using activated carbon adsorbent from locally available papaya peel biowaste. *J. Clean. Prod.* 118, 210–222. <https://doi.org/10.1016/j.jclepro.2016.01.054>

Aburto, J., Moran, M., Galano, A., Torres-García, E., 2015. Non-isothermal pyrolysis of pectin: A thermochemical and kinetic approach. *J. Anal. Appl. Pyrolysis* 112, 94–104. <https://doi.org/10.1016/j.jaap.2015.02.012>

Appel, C., Ma, L.Q., Rhue, R.D., Reve, W., 2008. Sequential sorption of lead and cadmium in three tropical soils. *Environ. Pollut.* 155, 132–140. <https://doi.org/10.1016/j.envpol.2007.10.026>

Atkins, P., Jones, L., 2010. *Chemical Principles: The Quest for Insight*, 5th ed. New York.

ATSDR, 2019. Substance Priority List. Agency Toxic Subst. Dis. Regist. URL <https://www.atsdr.cdc.gov/spl/index.html#2019spl>

- Boulaiche, W., Belhamdi, B., Hamdi, B., Trari, M., 2019. Kinetic and equilibrium studies of biosorption of M(II) (M = Cu, Pb, Ni, Zn and Cd) onto seaweed *Posidonia oceanica* fibers. *Appl. Water Sci.* 9, 173. <https://doi.org/10.1007/s13201-019-1062-1>
- Bulgariu, D., Bulgariu, L., 2016. Potential use of alkaline treated algae waste biomass as sustainable biosorbent for clean recovery of cadmium(II) from aqueous media: Batch and column studies. *J. Clean. Prod.* <https://doi.org/10.1016/j.jclepro.2015.05.124>
- Butterworth, C.A., Wallace, R.S., 2005. Molecular Phylogenetics of the Leafy Cactus Genus *Pereskia* (*Cactaceae*). *Syst. Bot.* 30, 800–808. <https://doi.org/10.1600/036364405775097806>
- Castillo, N.A.M., Ortega, E.P., Martínez, M.C.R., Ramos, R.L., Pérez, R.O., Alvarez, C.C., 2017. Single and competitive adsorption of Cd(II) and Pb(II) ions from aqueous solutions onto industrial chili seeds (*Capsicum annum*) waste. *Sustain. Environ. Res.* 27, 61–69. <https://doi.org/10.1016/j.serj.2017.01.004>
- Chen, S.B., Ma, Y.B., Chen, L., Xian, K., 2010. Adsorption of aqueous Cd<sup>2+</sup>, Pb<sup>2+</sup>, Cu<sup>2+</sup> ions by nano-hydroxyapatite: Single and multi-metal competitive adsorption study. *Geochem. J.* 44, 233–239. <https://doi.org/10.2343/geochemj.1.0065>
- Chen, Y.-G., Ye, W.-M., Yang, X.-M., Deng, F.-Y., He, Y., 2011. Effect of contact time, pH, and ionic strength on Cd(II) adsorption from aqueous solution onto bentonite from Gaomiaozi, China. *Environ. Earth Sci.* 64, 329–336. <https://doi.org/10.1007/s12665-010-0850-6>
- Cheng, S., Liu, Y., Xing, B., Qin, X., Zhang, C., Xia, H., 2021. Lead and cadmium clean removal from wastewater by sustainable biochar derived from poplar saw dust. *J. Clean. Prod.* 314, 128074. <https://doi.org/10.1016/j.jclepro.2021.128074>
- Coelho, G.F., Gonçalves, A.C., Schwantes, D., Rodríguez, E.Á., Tarley, C.R.T., Dragunski, D., Conradi Junior, É., 2018. Removal of Cd(II), Pb(II) and Cr(III) from water using modified residues of *Anacardium occidentale* L. *Appl. Water Sci.* 8, 1–21. <https://doi.org/10.1007/s13201-018-0724-8>
- Coelho, G.F., Gonçalves, A.C., Tarley, C.R.T., Casarin, J., Nacke, H., Francziskowski, M.A., 2014. Removal of metal ions Cd (II), Pb (II), and Cr (III) from water by the cashew nut shell *Anacardium occidentale* L. *Ecol. Eng.* 73, 514-525. <https://doi.org/10.1016/j.ecoleng.2014.09.103>
- Cruz, T.M., Santos, J.S., do Carmo, M.A.V., Hellström, J., Pihlava, J.M., Azevedo, L., Granato, D., Marques, M.B., 2021. Extraction optimization of bioactive compounds from ora-pro-nobis (*Pereskia aculeata* Miller) leaves and their in vitro antioxidant and antihemolytic activities. *Food Chem.* 361, 130078. <https://doi.org/10.1016/j.foodchem.2021.130078>
- Dutta, A., Zhou, L., Castillo-Araiza, C.O., De Herdt, E., 2016. Cadmium(II), Lead(II), and Copper(II) Biosorption on Baker's Yeast (*Saccharomyces cerevesiae*). *J. Environ. Eng.* 142, 1–7. [https://doi.org/10.1061/\(ASCE\)EE.1943-7870.0001041](https://doi.org/10.1061/(ASCE)EE.1943-7870.0001041)
- Elias, M.M.C., Soares, L.C., Maia, L.C., Dias, M.V.L., Gurgel, L.V.A., 2022. Multivariate optimization applied to the synthesis and reuse of a new sugarcane bagasse-based biosorbent to remove Cd(II) and Pb(II) from aqueous solutions. *Environ. Sci. Pollut. Res.* <https://doi.org/10.1007/s11356-022-18654-9>
- Fomina, M., Gadd, G.M., 2014. Biosorption: Current perspectives on concept, definition and application. *Bioresour. Technol.* 160, 3–14. <https://doi.org/10.1016/j.biortech.2013.12.102>

Guo, X., Zhang, S., Shan, X., 2008. Adsorption of metal ions on lignin. *J. Hazard. Mater.* 151, 134–142. <https://doi.org/10.1016/j.jhazmat.2007.05.065>

He, J., Chen, J.P., 2014. A comprehensive review on biosorption of heavy metals by algal biomass: Materials, performances, chemistry, and modeling simulation tools. *Bioresour. Technol.* 160, 67–78. <https://doi.org/10.1016/j.biortech.2014.01.068>

Jiao, G.-J., Ma, J., Li, Y., Jin, D., Zhou, J., Sun, R., 2022. Removed heavy metal ions from wastewater reuse for chemiluminescence: Successive application of lignin-based composite hydrogels. *J. Hazard. Mater.* 421, 126722. <https://doi.org/10.1016/j.jhazmat.2021.126722>

Jimenez, R.S., Dal Bosco, S.M., Carvalho, W.A., 2004. Remoção de metais pesados de efluentes aquosos pela zeólita natural escolecita - influência da temperatura e do pH na adsorção em sistemas monoelementares. *Quim. Nova* 27, 734–738. <https://doi.org/10.1590/S0100-40422004000500011>

Jones, B.O., John, O.O., Luke, C., Ochieng, A., Bassey, B.J., 2016. Application of mucilage from *Dicerocaryum eriocarpum* plant as biosorption medium in the removal of selected heavy metal ions. *J. Environ. Manage.* 177, 365–372. <https://doi.org/10.1016/j.jenvman.2016.04.011>

Karthikeyan, S., Balasubramanian, R., Iyer, C.S.P., 2007. Evaluation of the marine algae *Ulva fasciata* and *Sargassum* sp. for the biosorption of Cu(II) from aqueous solutions. *Bioresour. Technol.* 98, 452–455. <https://doi.org/10.1016/j.biortech.2006.01.010>

Kim, H.S., Kim, Y.J., Seo, Y.R., 2015. An Overview of Carcinogenic Heavy Metal: Molecular Toxicity Mechanism and Prevention. *J. Cancer Prev.* 20, 232–240. <https://doi.org/10.15430/jcp.2015.20.4.232>

Klemm, D., Philipp, B., Heinze, T., Heinze, U., Wagenknecht, W., 1998. *Comprehensive Cellulose Chemistry: Functionalization of Cellulose*. New York: Wiley-VCH.

Li, Q., Song, H., Han, R., Wang, G., Li, A., 2019. Efficient removal of Cu(II) and citrate complexes by combined permanent magnetic resin and its mechanistic insights. *Chem. Eng. J.* 366, 1–10. <https://doi.org/10.1016/j.cej.2019.02.070>

Low, K., Lee, C., Liew, S., 2000. Sorption of cadmium and lead from aqueous solutions by spent grain. *Process Biochem.* 36, 59–64. [https://doi.org/10.1016/S0032-9592\(00\)00177-1](https://doi.org/10.1016/S0032-9592(00)00177-1)

Maciel, V.B.V., Yoshida, C.M.P., Boesch, C., Goycoolea, F.M., Carvalho, R.A., 2020. Iron-rich chitosan-pectin colloidal microparticles laden with ora-pro-nobis (*Pereskia aculeata* Miller) extract. *Food Hydrocoll.* 98, 105313. <https://doi.org/10.1016/j.foodhyd.2019.105313>

Maciel, V.B.V., Yoshida, C.M.P., Goycoolea, F.M., 2018. Agronomic Cultivation, Chemical Composition, Functional Activities and Applications of *Pereskia* Species – A Mini Review. *Curr. Med. Chem.* 26, 4573–4584. <https://doi.org/10.2174/0929867325666180926151615>

Mahmood-ul-Hassan, M., Suthor, V., Rafique, E., Yasin, M., 2015. Removal of Cd, Cr, and Pb from aqueous solution by unmodified and modified agricultural wastes. *Environ. Monit. Assess.* 187, 19. <https://doi.org/10.1007/s10661-014-4258-8>

Maia, L.C., Soares, L.C., Alves Gurgel, L.V., 2021. A review on the use of lignocellulosic materials for arsenic adsorption. *J. Environ. Manage.* 288, 112397. <https://doi.org/10.1016/j.jenvman.2021.112397>

Marques Neto, J. de O., Bellato, C.R., Milagres, J.L., Pessoa, K.D., Alvarenga, E.S. de, 2013. Preparation and evaluation of chitosan beads immobilized with Iron(III) for the removal of As(III) and As(V) from water. *J. Braz. Chem. Soc.* 24, 121–132. <https://doi.org/10.1590/S0103-50532013000100017>

Martin, A.A., de Freitas, R.A., Sasaki, G.L., Evangelista, P.H.L., Sierakowski, M.R., 2017. Chemical structure and physical-chemical properties of mucilage from the leaves of *Pereskia aculeata*. *Food Hydrocoll.* 70, 20–28. <https://doi.org/10.1016/j.foodhyd.2017.03.020>

McBride, M.B., 1994. *Environmental Chemistry of Soils*. New York: Oxford University Press. <https://doi.org/10.2134/jeq1995.00472425002400010029x>

McBride, M.B., 1989. Reactions Controlling Heavy Metal Solubility in Soils. In: *Advances in Soil Science*. New Brunswick, pp. 1–56. [https://doi.org/10.1007/978-1-4613-8847-0\\_1](https://doi.org/10.1007/978-1-4613-8847-0_1)

Mi, X., Huang, G., Xie, W., Wang, W., Liu, Y., Gao, J., 2012. Preparation of graphene oxide aerogel and its adsorption for Cu<sup>2+</sup> ions. *Carbon N. Y.* 50, 4856–4864. <https://doi.org/10.1016/j.carbon.2012.06.013>

Neves, I.C.O., Rodrigues, A.A., Valentim, T.T., Meira, A.C.F. de O., Silva, S.H., Alcântara, L.A., de Resende, J.V., 2020. Amino acid-based hydrophobic affinity cryogel for protein purification from *ora-pro-nobis* (*Pereskia aculeata* Miller) leaves. *J. Chromatogr. B* 1161, 122435. <https://doi.org/10.1016/j.jchromb.2020.122435>

Nightingale, E.R., 1959. Phenomenological Theory of Ion Solvation. Effective Radii of Hydrated Ions. *J. Phys. Chem.* 63, 1381–1387. <https://doi.org/10.1021/j150579a011>

Noh, J.S., Schwarz, J.A., 1990. Effect of HNO<sub>3</sub> treatment on the surface acidity of activated carbons. *Carbon N. Y.* 28, 675–682. [https://doi.org/10.1016/0008-6223\(90\)90069-B](https://doi.org/10.1016/0008-6223(90)90069-B)

Oliveira, N.L., Rodrigues, A.A., Oliveira Neves, I.C., Teixeira Lago, A.M., Borges, S.V., de Resende, J.V., 2019. Development and characterization of biodegradable films based on *Pereskia aculeata* Miller mucilage. *Ind. Crops Prod.* 130, 499–510. <https://doi.org/10.1016/j.indcrop.2019.01.014>

Papageorgiou, S.K., Katsaros, F.K., Kouvelos, E.P., Nolan, J.W., Le Deit, H., Kanellopoulos, N.K., 2006. Heavy metal sorption by calcium alginate beads from *Laminaria digitata*. *J. Hazard. Mater.* 137, 1765–1772. <https://doi.org/10.1016/j.jhazmat.2006.05.017>

Pavia, D.L., Lampman, G.M., Kriz, G.S., 2014. *Introduction to Spectroscopy*, 5<sup>th</sup> edition. Thomson Learning, Inc.

Pearson, R.G., 1990. Hard and soft acids and bases - the evolution of a chemical concept. *Coord. Chem. Rev.* 100, 403–425. [https://doi.org/10.1016/0010-8545\(90\)85016-L](https://doi.org/10.1016/0010-8545(90)85016-L)

Pehlivan, E., Altun, T., Cetin, S., Iqbal Bhangar, M., 2009. Lead sorption by waste biomass of hazelnut and almond shell. *J. Hazard. Mater.* 167, 1203–1208. <https://doi.org/10.1016/j.jhazmat.2009.01.126>

Pereira, A.R., Soares, L.C., Teodoro, F.S., Elias, M.M.C., Ferreira, G.M.D., Savedra, R.M.L., Siqueira, M.F., Martineau-Corcós, C., da Silva, L.H.M., Prim, D., Gurgel, L.V.A., 2020. Aminated cellulose as a versatile adsorbent for batch removal of As(V) and Cu(II) from mono- and multicomponent aqueous solutions. *J. Colloid Interface Sci.* 576, 158–175. <https://doi.org/10.1016/j.jcis.2020.04.129>

- Petrus, R., Warchoń, J., 2003. Ion exchange equilibria between clinoptilolite and aqueous solutions of  $\text{Na}^+/\text{Cu}^{2+}$ ,  $\text{Na}^+/\text{Cd}^{2+}$  and  $\text{Na}^+/\text{Pb}^{2+}$ . *Micropor. Mesopor. Mat.* 61, 137–146. [https://doi.org/10.1016/S1387-1811\(03\)00361-5](https://doi.org/10.1016/S1387-1811(03)00361-5)
- Puranik, P.R., Paknikar, K.M., 1999. Biosorption of Lead, Cadmium, and Zinc by *Citrobacter* Strain MCM B-181: Characterization Studies. *Biotechnol. Prog.* 15, 228–237. <https://doi.org/10.1021/bp990002r>
- Salman, S.M., Muhammad, S., e Shahwar, D., Iqbal, M., Aijaz, M., Siddique, M., Ali, A., Nawaz, S., Kamran, A.W., 2020. Biosorption of Pb(II) and Cd(II) ions from aqueous solution by chemically modified *Syzygium cumini* leaves and its equilibrium, kinetic and thermodynamic studies. *Pakistan J. Sci. Ind. Res. Ser. A Phys. Sci.* 63, 18–29. <https://doi.org/10.52763/pjsir.phys.sci.63.1.2020.18.29>
- Santos, T.J., Paggiaro, J., Cabral Silva Pimentel, H.D., Karla dos Santos Pereira, A., Cavallini, G.S., Pereira, D.H., 2022. Computational study of the interaction of heavy metal ions, Cd(II), Hg(II), and Pb(II) on lignin matrices. *J. Mol. Graph. Model.* 111, 108080. <https://doi.org/10.1016/j.jmgm.2021.108080>
- Serrano, S., Garrido, F., Campbell, C.G., García-González, M.T., 2005. Competitive sorption of cadmium and lead in acid soils of Central Spain. *Geoderma* 124, 91–104. <https://doi.org/10.1016/j.geoderma.2004.04.002>
- Souza, I.P.A.F., Cazetta, A.L., Pezoti, O., Almeida, V.C., 2017. Preparation of biosorbents from the Jatoba (*Hymenaea courbaril*) fruit shell for removal of Pb(II) and Cd(II) from aqueous solution. *Environ. Monit. Assess.* 189, 632. <https://doi.org/10.1007/s10661-017-6330-7>
- Sposito, G., 2008. *The Chemistry of Soils*, 2<sup>nd</sup> ed.. New York: Oxford University Press.
- Tan, Y., Wan, X., Zhou, T., Wang, L., Yin, X., Ma, A., Wang, N., 2022. Novel Zn-Fe engineered kiwi branch biochar for the removal of Pb(II) from aqueous solution. *J. Hazard. Mater.* 424, 127349. <https://doi.org/10.1016/j.jhazmat.2021.127349>
- Teodoro, F.S., Ramos, S.N. do C., Elias, M.M.C., Mageste, A.B., Ferreira, G.M.D., da Silva, L.H.M., Gil, L.F., Gurgel, L.V.A., 2016. Synthesis and application of a new carboxylated cellulose derivative. Part I: Removal of  $\text{Co}^{2+}$ ,  $\text{Cu}^{2+}$  and  $\text{Ni}^{2+}$  from monocomponent spiked aqueous solution. *J. Colloid Interface Sci.* 483, 185–200. <https://doi.org/10.1016/j.jcis.2016.08.004>
- Vanhoudt, N., Vandenhove, H., Leys, N., Janssen, P., 2018. Potential of higher plants, algae, and cyanobacteria for remediation of radioactively contaminated waters. *Chemosphere* 207, 239–254. <https://doi.org/10.1016/j.chemosphere.2018.05.034>
- Volesky, B., 2001. Detoxification of metal-bearing effluents: Biosorption for the next century. *Hydrometallurgy* 59, 203–216. [https://doi.org/10.1016/S0304-386X\(00\)00160-2](https://doi.org/10.1016/S0304-386X(00)00160-2)
- Yousaf, A., Athar, M., Salman, M., Farooq, U., Chawla, F.S., 2017. Biosorption characteristics of *Pennisetum glaucum* for the removal of Pb(II), Ni(II) and Cd(II) ions from aqueous medium. *Green Chem. Lett. Rev.* 10, 462–470. <https://doi.org/10.1080/17518253.2017.1402093>
- Zhao, G., 2011. Sorption of Heavy Metal Ions from Aqueous Solutions: A Review. *Open Colloid Sci. J.* 4, 19–31. <https://doi.org/10.2174/1876530001104010019>
- Zhou, Z., Xu, Z., Feng, Q., Yao, D., Yu, J., Wang, D., Lv, S., Liu, Y., Zhou, N., Zhong, M.-e., 2018. Effect of pyrolysis condition on the adsorption mechanism of lead, cadmium and copper on tobacco stem biochar. *J. Clean. Prod.* 187, 996–1005. <https://doi.org/10.1016/j.jclepro.2018.03.268>